



RESEARCH ARTICLE

STUDYING OF PROPORTIONAL INTEGRAL (RESET) CONTROL ON FLOW CHARACTERISTIC ON ORIFICE PLATE OF DIFFERENT FLUID SYSTEM

*C.P. Ukpaka, **C. U. Orji and *** T. C. Nwofor

*Department of Chemical/Petrochemical Engineering, Rivers State University of Science and Technology, Nkpolu, P.M.B. 5080, Port Harcourt, Nigeria

** Department of Marine Engineering, Rivers State University of Science and Technology, Nkpolu, P.M.B. 5080, Port Harcourt, Nigeria

**Department of Civil and Environmental Engineering, University of Port Harcourt, Nigeria

ARTICLE INFO

Article History:

Received 16th June, 2011
Received in revised form
19th July, 2011
Accepted 29th August, 2011
Published online 17th September, 2011

Key words:

Proportional,
Integral control,
Orifice plate,
Fluid, flow.

ABSTRACT

Model based on Bernoulli equation and coefficient of discharge as a function of the Reynolds number was applied at different levels in different fluid system in Industrial operation of orifice plate. The model was based on the principle of constant area, variable pressure drop. The experimental results obtained from the research work were used in monitoring and predicting the usefulness of pneumatic proportional integral (reset) control on flow characteristics of different fluid flowing through an orifice plate. Mathematical models were developed for both compressible and non compressible fluid in terms of flow rate as well related to the pneumatic proportional integral (Reset) control. The proportional and integral gain is one of the functional parameters that control and determine the effectiveness of the industrial operation of the system by reducing the error value for laminar and turbulent flow experienced by the orifice plate.

Copy Right, IJCR, 2011, Academic Journals. All rights reserved

INTRODUCTION

Instrumentation and process control can be traced back many millennia. The evolution of instrumentation and process control has undergone several industrial revolutions leading to the complexities of modern day microprocessor-controlled processing. (Ang, Cheng and Li, 2005; Aris, 1994; Bender, 2000; Liang, 2009; and Minorsky, 1922). Today's technological evolution has made it possible to measure parameters deemed impossible only a few years ago. Improvements in accuracy, tighter control, and waste reduction have also been achieved. An orifice plate is a device used for measuring the rate of fluid flow. It uses the same principle as a Venturi nozzle, namely Bernoulli's principle which states that there is a relationship between the pressure of the fluid and the velocity of the fluid. When the velocity increases, the pressure decreases and vice versa. Orifice plates are most commonly used for continuous measurement of fluid flow in pipes. (Geankoplis, 2003; Beguete, 2003; Rajpust, 1998; Raven, 2003; Eckman, 2005; Ogata, 1995; Wayne, 2006; Cunningham, 2001; and Ogoni and Ukpaka, 2004). They are also used in some small river systems to measure flow rates at locations where the river passes through a culvert

or drain. Only a small number of rivers are appropriate for the use of the technology since the plate must remain completely immersed i.e. the approach pipe must be full, and the river must be substantially free of debris. In the natural environment large orifice plates are used to control onward flow in flood relief dams. In these structures a low dam is placed across a river and in normal operation the water flows through the orifice plate unimpeded as the orifice is substantially larger than the normal flow cross section. However, in floods, the flow rate rises and floods out the orifice plate which can then only pass a flow determined by the physical dimensions of the orifice. Flow is then held back behind the low dam in a temporary reservoir which is slowly discharged through the orifice when the flood subsides (Zhang, Li. And Cheng, 2005; George and Austin, 1997; Eastop and McConkey, 1995; Octave, 1972; Holman, 1997 and Rose, 1963).

MATERIALS AND METHODS

The Concept of the Mathematical Model

An orifice plate is a thin plate with a hole in the middle. It is usually placed in a pipe in which fluid flows. When the fluid reaches the orifice plate, with the hole in the middle, the fluid is forced to converge to go through the small hole; the point of maximum convergence actually occurs shortly downstream of

*Corresponding author: chukwuemeka24@yahoo.com

the physical orifice, at the so-called vena contracta point (Fig 1). (Zhang and Li, 2004); Strout, 1995; Smith and Ness, 1999; Rose, 1963; Ogoni and Ukpaka, 2004 and Cunningham, 2001). As it does so, the velocity and the pressure changes. Beyond the vena contracta, the fluid expands and the velocity and pressure change once again. By measuring the difference in fluid pressure between the normal pipe section and at the vena contracta, the volumetric and mass flow rates can be obtained from Bernoulli's equation. The vena contracta, the fluid expands and the velocity and pressure change once again. By measuring the difference in fluid pressure between the normal pipe section and at the vena contracta, the volumetric and mass flow rates can be obtained from Bernoulli's equation.

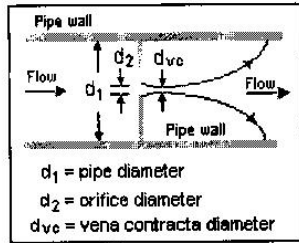


Fig. 1: Flat-plate, sharp-edge orifice

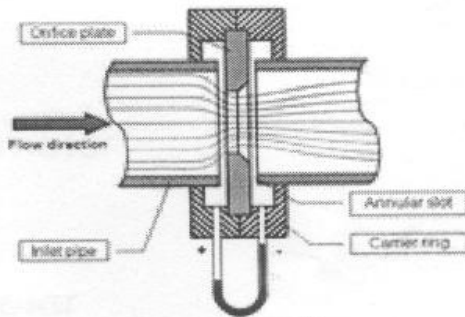


Fig. 2: Orifice plate

Design model of constant area variable pressure drop

The orifice flow equation is a key equation for hydraulic systems. Like pipe flow, fluid flow in orifices can be either laminar or turbulent (see Figure 1). In laminar flow, each fluid particle follows a well defined trajectory, with velocity only in the direction of flow. In turbulent flow (most common in systems due to small line diameters and small orifices) each particle flows in the general direction (velocity) of the flow, but is subjected to fluctuating cross current velocities. Equations for computing orifice flow are different for laminar and turbulent flow.

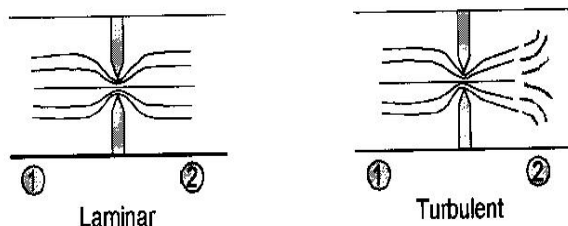


Fig. 3: Flow streamlines for laminar and turbulent orifice flow

Determination of laminar or turbulent is determined using the

Reynolds number, as given; $Re = \frac{\rho^{vd} h}{\mu} = \frac{vd h}{\nu}$ (1)

For low values of Re, flow is laminar. For high values of Re, flow is turbulent. From Bernoulli's equation, the total energy loss is the energy converted to heat by friction of particles against the wall each other is presented as;

$\Delta p = (p_1 + 1/2 \rho v_1^2 + \rho g z_1) - (p_2 + 1/2 \rho v_2^2 + \rho g z_2)$ (2)

Assuming, away from orifice, that $v_1 = v_2$ and $A_1 = A_2$, the flow becomes a product of the area and speed as presented in equation (3)

$Q = Av = A \sqrt{\frac{2}{\rho \xi}} (p_1 - p_2)$ (3)

Where ξ is a dimensionless loss coefficient, representing the energy loss associated with the pressure drop. For hydraulic systems, this equation is normally written as

$Q = a_d A \sqrt{\frac{2}{\rho}} (p_1 - p_2)$ (4)

Where a_d is the discharge coefficient and represents the energy loss in the fluid. Equation (4) is the orifice flow equation. The discharge coefficient is the key element to estimate for laminar and turbulent flow regimes. Inspection of the equation (4) indicates that the flow rate varies proportionally with area if the Δp is held constant, and that the flow rate varies with the square root of tip if the flow area is held constant. Figure 4 shows notional charts of the flow behavior. Δp is assumed constant

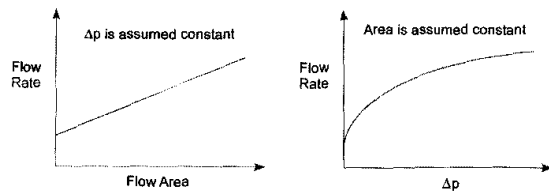


Fig. 4: Flow Rate Behavior for an Orifice

Turbulent Orifice Flow

For a sharp edge orifice, with turbulent flow and with orifice flow area, $A_0 \ll A$ (pipe flow area), the theoretical a_d is given as

$\alpha_d = \pi / (\pi + 2) = 611$ (5)

For short tube orifices of length L, pipe diameter d, and orifice diameter d_o , can be expressed as;

$a_d = \left(2.28 + 64 \frac{2L}{d_o d} \right)^{-1/2}$ for $\frac{d_o d}{2L} \leq 50$ (6)

$a_d = \left[1.5 + 13.74 \left(\frac{2L}{d_o d} \right)^{1/2} \right]^{-1/2}$ for $\frac{d_o d}{2L} > 50$ (7)

Laminar Orifice Flow

Equation (4) can be used in the turbulent-laminar (transition) region and the laminar flow region using the expression presented below as;

$$a_d = \delta \sqrt{Re} \quad (8)$$

where

$$\delta = \frac{a_{d,turb}}{\sqrt{Re_{crit}}} = \frac{0.611}{\sqrt{20}} \approx 0.137 \text{ (sharp edged orifice)} \quad (9)$$

$$\delta = \frac{a_{d,turb}}{\sqrt{Re_{crit}}} = \frac{0.611}{\sqrt{80}} \approx 0.068 \text{ (rounded off orifice)} \quad (10)$$

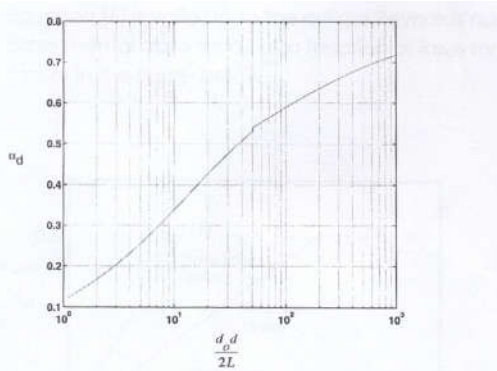


Fig. 5: Turbulent Flow Discharge Coefficient for Short Tube Orifice

δ called the laminar flow coefficient and depends on orifice geometry. $a_{d,turb}$ comes from equation (8). Re_{15} the critical (breakpoint) Reynolds number found during empirical testing for the type of orifice as presented Figure 3. These equations are theoretical, but have been validated by experiment. Equation (9) is valid up to the critical Reynolds number as shown in Figure 5. Experimental data for a function of α_d and Re_c for various orifices are shown in the Figure 5 below.

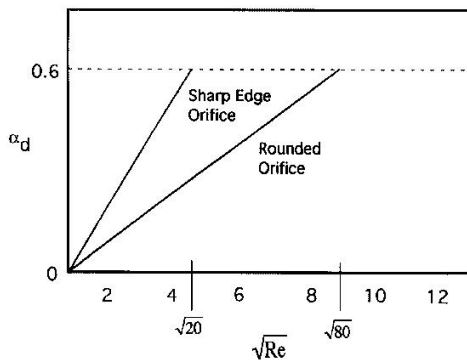


Fig. 6: Laminar Flow Discharge Coefficient for Orifices

The sloped lines can be used for α_d in the laminar flow region. At the breakpoint, turbulent flow occurs and $\alpha_d = 0.6$.

Incompressible Flow Through an Orifice

By assuming steady-state, incompressible (constant fluid density), in viscous, laminar flow in a horizontal pipe (no change in elevation) with negligible frictional losses, Bernoulli's equation reduces to an equation relating the conservation of energy between two points on the same streamline; the mathematical expression is given as;

$$P_1 + \frac{1}{2} \cdot \rho \cdot V_1^2 = P_2 + \frac{1}{2} \cdot \rho \cdot V_2^2 \quad (11)$$

Thus, equation (11) can be written as

$$P_1 - P_2 = \frac{1}{2} \cdot \rho \cdot V_2^2 - \frac{1}{2} \cdot \rho \cdot V_1^2 \quad (12)$$

By continuity equation we have

$$Q = A_1 \cdot V_1 = A_2 \cdot V_2 \quad (13)$$

$$V_1 = Q/A_1 \text{ and } V_2 = Q/A_2: \quad (13a)$$

Therefore equation (13) can be written as

$$P_1 - P_2 = \frac{1}{2} \cdot \rho \cdot \left(\frac{Q}{A_2} \right)^2 - \frac{1}{2} \cdot \rho \cdot \left(\frac{Q}{A_1} \right)^2 \quad (14)$$

Solving for Q from equation (14) we have

$$Q = A_2 \sqrt{\frac{2(P_1 - P_2)/\rho}{1 - (A_2/A_1)^2}} \quad (15)$$

and

$$Q = A_2 \sqrt{\frac{1}{1 - \left(\frac{d_2}{d_1} \right)^4}} \sqrt{2(P_1 - P_2)/\rho} \quad (16)$$

The above expression for Q gives the theoretical volume flow rate. Introducing the beta factor $\beta = \frac{d_2}{d_1}$ as well as the coefficient of discharge C_d :

$$Q = C_d A_2 \sqrt{\frac{1}{1 - \beta^4}} \sqrt{2(P_1 - P_2)/\rho} \quad (17)$$

And finally introducing the meter coefficient C which is defined as

$$C = \frac{C_d}{\sqrt{1 - \beta^4}} \quad (18)$$

to obtain the final equation for the volumetric flow of the fluid through the orifice:

$$Q = CA_2 \sqrt{2(P_1 - P_2)/\rho} \quad (19)$$

Multiplying by the density of the fluid to obtain the equation for the mass flow rate at any section in the pipe; using equation (19) we have the expression presented in equation (20)

$$\dot{m} = \rho Q = CA_2 \sqrt{2\rho(P_1 - P_2)} \quad (20)$$

Deriving the above equations using the cross-section of the orifice opening and is not as realistic as using the minimum cross-section at the vena contracta. In addition, frictional losses may not be negligible and viscosity and turbulence effects may be present. For that reason, the coefficient of discharge C_d is introduced. Methods exist for determining the coefficient of discharge as a function of the Reynolds number.

The parameter $\sqrt{1 - \beta^4}$ is often referred to as the velocity of approach factor and dividing the coefficient of discharge by that parameter (as was done above) produces the flow coefficient C. Methods also exist for determining the flow coefficient as a function of the beta function β and the location of the downstream pressure sensing tap. For rough approximations, the flow coefficient may be assumed to be between 0.60 and 0.75. For a first approximation, a flow coefficient of 0.62 can be used as this approximates to fully

developed flow. An orifice orgy works well when supplied with a fully developed flow profile. This is achieved by a long upstream length (20 to 40 pipe diameters, depending on Reynolds number) or the use of a flow conditioner. Orifice plates are small and inexpensive but do not recover the pressure drop as well as a venture nozzle does. If space permit, a venturi meter is more efficient than a flow meter,

Flow of Gases Through an Orifice

In general equation (20) is applicable only for incompressible flows. It can be modified by introducing the expansion factor Y to account for the compressibility of gases.

$$\dot{m} = \rho_1 Q = C Y A_2 \sqrt{2 \rho_1 (P_1 - P_2)} \tag{21}$$

Y is 1.0 for incompressible fluids and it can be calculated for compressible gases

Calculation of expansion factor

The expansion factor, which allows for the change in the density of an ideal gas as it expands isentropically, is given as:

$$Y = \sqrt{r^{2/k} \left(\frac{k}{k-1}\right) \left(\frac{1-r(k-1)/k}{1-r}\right) \left(\frac{11-\beta^4}{1-\beta^4 r^2/k}\right)} \tag{22}$$

For values of β less than 0.25, β^4 approaches 0 and the last bracketed term in the above equation approaches 1. Thus, for the large majority of orifice plate installations: the expression is given as

$$Y = \sqrt{r^{2/k} \left(\frac{k}{k-1}\right) \left(\frac{1-r(k-1)/k}{1-r}\right)} \tag{23}$$

Substituting equation (4) into the mass flow rate equation (3):

$$\dot{m} = C A_2 \sqrt{2 \rho_1 \left(\frac{k}{k-1}\right) \left[\frac{\left(P_2/P_1\right)^{2/k} \left(P_2/P_1\right)^{(k+1)/k}}{1-P_2/P_1}\right] (P_1 - P_2)} \tag{24}$$

and

$$\dot{m} = C A_2 \sqrt{2 \rho_1 \left(\frac{k}{k-1}\right) \left[\frac{\left(P_2/P_1\right)^{2/k} \left(P_2/P_1\right)^{(k+1)/k}}{\left(P_2/P_1\right)/P_1}\right] (P_1 - P_2)} \tag{25}$$

and thus, the final equation for the non-choked (i.e., sub-sonic) flow of ideal gases through an orifice for values of β less than 0.25 is given as;

$$\dot{m} = C A_2 \sqrt{2 \rho_1 P_1 \left(\frac{k}{k-1}\right) \left[\left(P_2/P_1\right)^{2/k} \left(P_2/P_1\right)^{(k+1)/k}\right]} \tag{26}$$

Using the law of compressibility factor (which corrects for non-ideal gases), a practical equation is obtained for the non-choked flow of real gases through an orifice for values of β less than 0.25

$$\dot{m} = C A_2 P_1 \sqrt{\frac{2 M}{Z R T_1} \left(\frac{k}{k-1}\right) \left[\left(P_2/P_1\right)^{2/k} \left(P_2/P_1\right)^{(k+1)/k}\right]} \tag{27}$$

Recalling that $Q_1 = \frac{\dot{m}}{\rho_1}$ and $\rho_1 = M \frac{P_1}{Z R T_1}$ (Ideal gas law and the compressibility factor)

Therefore substituting this conditions into equation (27) we have

$$Q_1 = C A_2 \sqrt{2 \frac{Z R T_1}{M} \left(\frac{k}{k-1}\right) \left[\left(P_2/P_1\right)^{2/k} - \left(P_2/P_1\right)^{(k+1)/k}\right]} \tag{28}$$

A detailed explanation of choked and non-choked flow of gases, as well as the equation for the choked flow of gases through restriction orifices is available in the literatures. The flow of real gases through thin-plate orifices never becomes fully choked. ‘‘Cunningham (1951) first drew attention to the fact that choked flow will not occur across a standard, thin, square-edged orifice.’’¹¹ The mass flow rate through the orifice continues to increase as the downstream pressure is lowered to a perfect vacuum, though the mass flow rate increases slowly as the downstream pressure is reduced below the critical pressure.

Permanent Pressure Drop for Incompressible Fluids

For a square-edge orifice plate with flange taps

$$\frac{\Delta P_p}{\Delta P_i} = 1 - 0.24\beta - 0.52\beta^2 - 0.16\beta^3 \tag{29}$$

The equation (29) obtained is a polynomial expression and if the change in pressure of the left hand side is known the above expression in equation (29) can be solved mathematical to establish the values of β

Mathematical model (calculations)

Recalling the mathematical model that define the theoretical flow rate in relationship with pressure and other functional parameters.

$$\text{Let } Qt = \frac{A_{orif}}{\sqrt{1 - (A_{orif} / Ap)^2}} \sqrt{\frac{2(p_1 - p_2)}}{\rho}} \tag{30}$$

$$\sqrt{\frac{2(p_1 - p_2)}}{\rho} = \frac{Q}{A_{orif}} \sqrt{1 - (A_{orif} / Ap)^2} \tag{31}$$

$$(p_1 - p_2) = \left(\frac{Q}{A_{orif}}\right)^2 \left(\frac{\rho}{2}\right) \left(1 - (A_{orif} / Ap)^2\right) \tag{32}$$

$$\Delta P = \left(Q / A_{orif}\right)^2 \left(\frac{\rho}{2}\right) \left[1 - \frac{A_{orif}^2}{Ap^3}\right] \tag{33}$$

Recalling the mathematical model that expressed the flow rate in relation to change in pressure, radius of the pipe, length and π as show in equation (35) is given as

$$Q = \frac{6\pi r^4 \Delta P}{8L\pi} \Leftrightarrow \pi = \frac{6\pi r^4 \Delta P}{8LQ} \tag{34}$$

$$\text{We have } A = \frac{\pi r^2}{4}$$

$$r = 2\sqrt{(A/\pi)} = 5.29$$

Correlation of developed Model with Proportional

$$\text{Let } Qt = \frac{A_{orif}}{\sqrt{1 - (A_{orif} / Ap)^2}} \sqrt{\frac{2(p_1 - p_2)}}{\rho}} \tag{36}$$

$$(P_1 - P_2) = \left(\frac{Q}{A_{orif}} \right)^2 \left(\frac{\rho}{2} \right) \left[1 - \frac{A_{orif}^2}{A_p^2} \right] \quad (37)$$

$$\text{Also } P = P^o + K_c E + K_1 \int_0^t E dt \quad (38)$$

There is one common factor $P_2 - P_1$ in the 2 equations thus we have (i.e $P_1 - P_2 = P - P_o$) therefore combing equation

$$\frac{\rho \times Q_t^2}{2 A_{orif}^2} \left[1 - \left(\frac{A_{orif}^2}{A_p^2} \right) \right] = - K_c E - K_1 \int_0^t E dt \quad (39)$$

$$\rho Q_t^2 \left[1 - \left(\frac{A_{orif}^2}{A_p^2} \right) \right] = - 2 A_{orif}^2 E \left[K_c + K_1 \int_0^t dt \right] \quad (40)$$

$$Q_t = \sqrt{\frac{2 A_{orif}^2 E (K_c + K_1 t)}{\rho \left[1 - \left(\frac{A_{orif}^2}{A_p^2} \right) \right]}} \quad (41)$$

Computational Procedure

The following parameters were used in evaluating the functional parameters that govern flow principles such as Q_t theoretical flow rate $Q_t = 2$ to $5 \text{ m}^3/\text{sec}$, cross sectional area of the orifice $A_{roif} = 22 \text{ cm}^2$, cross sectional area of the pipe diameter $A_p = 88 \text{ cm}$, error (E) = 1.0, density of water $\rho = 1000 \text{ kg/m}^3$, density of ethylene glycol $\rho = 1113 \text{ kg/m}^3$ and density of glycerol $\rho = 126 \text{ kg/m}^3$.

RESULTS AND DISCUSSION

The results obtained from the research works are presented in Tables and Figures. At the end of this research work we can in confidence that the rate of flow for the constant area variable pressure drop increases with increase in pressure difference, time, and viscosity with respect to the increase in density of the fluid therefore the rate of flow is proportional to change in pressure, viscosity, and time. The theoretical computation of the change in pressure and proportional and integral gain are presented in the Appendix.

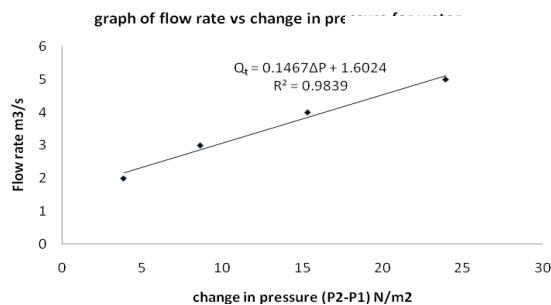


Fig. 7: Graph of flow rate vs change in pressure for water

Figure 7 illustrates the relationship between the flow rate and change in pressure for water. Increase in flow rate was observed with increase in pressure change. The variation in flow rate can be attributed to the variation in change of

pressure. The polynomial equation is given as $Q_t = 0.1467 \Delta p + 1.6024$ with the equation of the root as, $R^2 = 0.9839$.

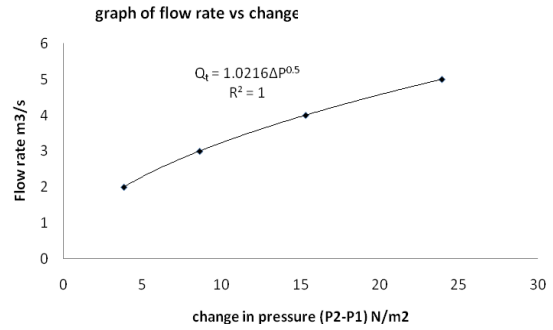


Fig. 8: Graph of flow rate vs change in pressure for water

The variation in flow rate upon the influence of variation of change in pressure is illustrated in Figure 8. The graph shown in Figure 8 illustrates increase in flow rate with increase in change of pressure. The power index equation is given as $Q_t = 1.0216 \Delta p^{0.5}$ with $R^2 = 1$, for water .

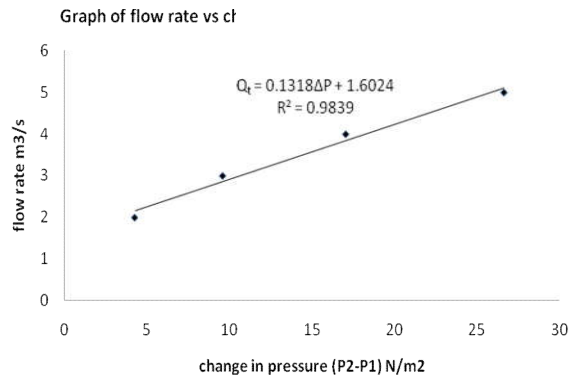


Fig. 9: Graph of flow rate vs change in pressure for ethylene glycol

Figure 9 illustrates the flow rate versus change in pressure for ethylene glycol. The variation in the flow rate can be attributed to the variation in change of pressure in the process. Increase in flow rate resulted to increase in change in pressure with it polynomial expression given as $Q_t = 0.1318 \Delta p + 1.6024$ with $R^2 = 0.9839$.

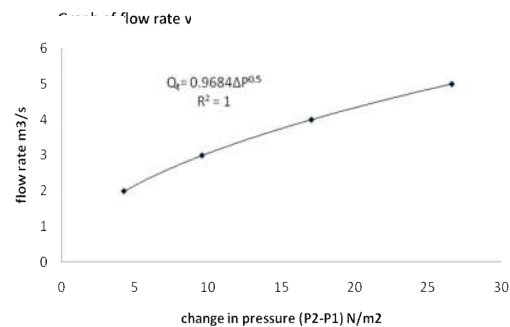


Fig. 10: Graph of flow rate vs change in pressure for glycol

It is seen that from Figure 10, flow rate increases with increase in change in pressure for ethylene glycol. The variation in flow rate can be attributed to the variation in change in

pressure. The power index mathematical equation is expressed as $Q_t = 0.9684 \Delta p^{0.5}$ with $R^2 = 1$.

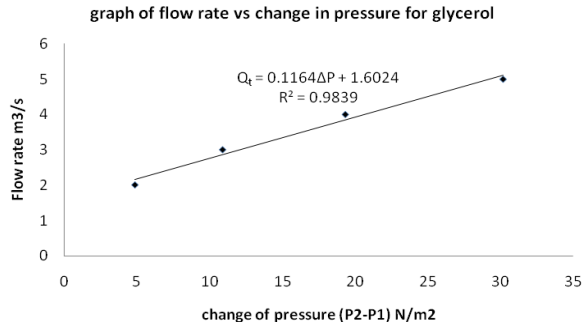


Fig. 11: Graph of flow rate vs change in pressure for glycerol

Figure 11, illustrates the flow rate characteristics of glycerol against pressure of glycerol in pipe system. The variation in the flow rate glycerol can be attributed to the variation in change in pressure. The polynomial expression of the above curve as presented in Figure 11 is given as $Q_t = 0.1164 \Delta p + 1.6024$ with $R^2 = 0.9839$.

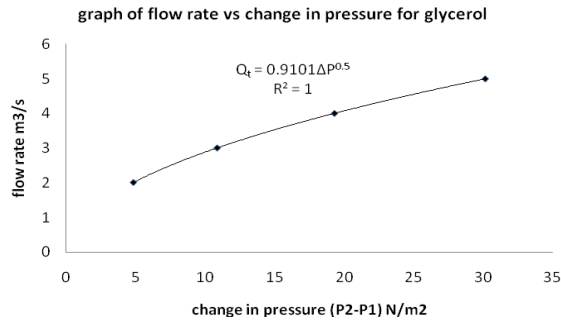


Fig. 12: Graph of flow rate vs change in pressure for glycerol

Figure 12 illustrates the flow rate characteristics of glycerol versus change in pressure for glycerol. Increase in flow rate characteristics was observed with increase in change in pressure. The variation in the flow rate characteristics can be attributed to the variation in change in pressure of the glycerol. The power index mathematical expression for the curve obtained Figure 12 is given as $Q_t = 0.9101 \Delta p^{0.5}$ with $R^2 = 1$.

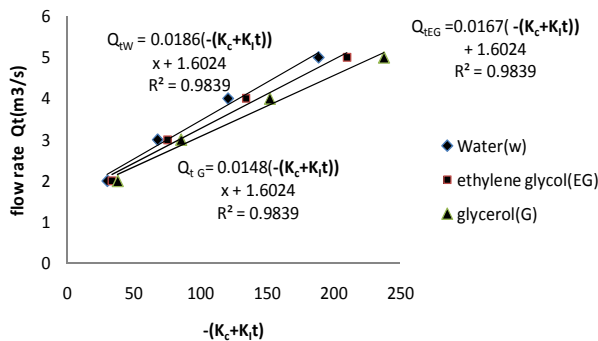


Fig. 13: Graph of flow rate vs gains for different fluids in system

Figure 13 illustrates the flow rate characteristics of different fluids system. The variation in flow rate can be attributed to the variation in the different gain inserted in the system as shown in Figure 13. Increase in flow rate was observed with increase in proportional and integral an (K_c, K_i) for water, ethylene glycol and glycerol. The mathematical expression for the different graphs as presented in Figure 13 is given as $Q_{tw} = 0.0186 (- (K_c + K_i t)) + 1.6024$ with $R^2 = 0.9839$, $Q_{tEG} = 0.0167 (- (K_c + K_i t)) + 1.6024$ with $R^2 = 0.9839$ and $Q_{tG} = 0.0148 (- (K_c + K_i t)) + 1.6024$ with $R^2 = 0.9839$ for water (w) ethylene (EG) and glycerol (G).

Conclusion

It can be noted that Accuracy in measurements limits the meter to a range of 3:1. The orifice has a relatively large permanent pressure loss that must be made up by the pumping machinery. To summarize, the orifice is the simplest, cheapest, easiest to replace, least accurate, more subject to damage and erosion, and has the highest loss and compared to other once which have more difficult to replace, most expensive, most accurate, has high tolerance to damage and erosion, and the lowest losses of all the three tubes (venturi-tube). The flow nozzle is intermediate between the other two and offers a good compromise. The Dall tube has the advantage of having the lowest insertion loss but cannot be used with slurries.

The proportional integral (reset) control process can be used to solubilize the flow characteristics of different fluids upon the influence of orifice plate. This innovative process has the potential to be used not only in a simple river flowing process bur also for industrial valuable resources process. At lower flow rate regimes ($1\text{m}^3/\text{s}$), the proportional integral gain increases linearly with increase in flow rate for water, ethylene glycol and glycerol. However, a polynomial expression were obtained in relation among the flow rate characteristics and the different fluids in system. The mathematical equations obtained in term of flow rate characteristics for the different fluids is given as

$$Q_{tw} = 0.0186 (- (K_c + K_i t)) + 1.6024 \text{ with } R^2 = 0.9839,$$

$$Q_{tEG} = 0.0167 (- (K_c + K_i t)) + 1.6024 \text{ with } R^2 = 0.9839$$

$$\text{and } Q_{tG} = 0.0148 (- (K_c + K_i t)) + 1.6024 \text{ with } R^2 = 0.9839$$

At different flow rate the response time can be evaluated using the developed polynomial expression as presented in this paper.

Nomenclature

$$d_h = \frac{4A}{S} \quad \text{hydraulic diameter (mm)}$$

$$A = \text{flow section area (m}^2\text{)}$$

$$S = \text{flow section perimeter}$$

$$V = \text{flow velocity (m/s}^2\text{)}$$

$$\mu = \text{dynamic viscosity (Ns/m}^2\text{)}$$

$$\nu = \text{kinematic viscosity (Ns/m}^2\text{)}$$

$$\Delta P_p = \text{permanent pressure drop}$$

$$\Delta P_1 = \text{indicated pressure drop at the flange taps (N/m}^2\text{)}$$

$$\beta = d_2/d_1 \text{ (dimensionless)}$$

$$K = \text{Specific heat ratio (C}_p\text{/C}_v\text{), dimensionless}$$

$$Q_1 = \text{upstream real gas flow rate, (m}^3\text{/s)}$$

C	=	orifice flow coefficient, (dimensionless)
A_2	=	cross-sectional area of the orifice hole, (m^2)
ρ_1	=	upstream real gas density, (kg/m^3)
P_1	=	upstream gas pressure, Pa with dimensions of (kg/ms^2)
P_2	=	downstream pressure, Pa with dimensions of (kg/ms^2)
M	=	the gas molecular mass. kg/mol (also known as the molecular weight)
R	=	the Universal Gas Law Constant = 8.3145 J/(mol K)
T_1	=	absolute upstream gas temperature, (K or °C)
Z	=	the gas compressibility factor at P and T_1 , (dimensionless)
r	=	radius of the pipe (mm)
L	=	length of the pipe (mm)
D	=	diameter of the pipe (mm)
η	=	viscosity of the fluid

REFERENCES

- Ang, K.H; Cheng G. C.Y and Li, Y (2005) PID Control System Analysis, Design and Technology, *IEE Trans Control System*, Vol. 13, No. 4, pp. 559-576.
- Aris, R.F (1994). Mathematical Modeling Techniques McGraw-Hill, new York, pp.3-9
- Beguete, W (2003). Process Control, Modeling , Design and Simulation, 5th edition, Asoke Ghosh, PHI Private Limited, pp.3-71.
- Bender, E. A. (2000). An Introduction to Mathematical Modeling, McGraw-Hill, New York pp, 127-300.
- Bennett, S. (1993). A History of Control Engineering McGraw-Hill, New York, pp.
- Cunningham, R.G (2001). Orifice Meters with Supercritical Compressible Flow. *Trans ASME* Vol, 73. pp.271-283.
- Eastop T.N and McConkey, (1995). Applied Thermodynamics for Engineering Technology, 5th edition, Longman, pp 33-41.
- Eckman, D.P (2005). Automatic Process Control, 2nd edition, Wiley Eastern, New Delhi, pp.27-30.
- Geankoplis, C.J (2003). Transport Process and Separation Process Principles. 4th edition Adoke G hosh, PHI Private Limited, pp. 41-61.
- George T and Austin, S. (1997). Chemical Process Industry, 5th edition, McGraw –Hill, pp. 533-757.
- Holman, J.P (1997). Heat Transfer, 8th edition, McGraw-Hill, pp. 2-30
- Liang Y. L (2009). Controlling Fuel Analysis on Using Computational Valve Controllers, McGraw-Hill, New York, p.10.
- Minorsky, N. (1922). Directional Stability Automatically steered Bocties. *Journal of American Social Naval Engineering*, Vol, 3, No. 2, pp. 280-300.
- Octave, L.S (1972).Chemical Reaction Engineering, 2nd edition, John Wiley and Sons, pp. 9-218.
- Ogata, K (1995). Modern Control Engineering, 2nd edition, Prentice Hall of India, new Delhi, pp. 72-80.
- Ogoni, H.A and Ukpaka, C.P. (2004). Instrumentation, Process Control and Dynamics. 1st edition, library of Congress Cataloging in Publication data pp.1-50
- Rajput, R.K (1998). Fluid Mechanics and Hydrualic Machines in S.I Unit. 3rd edition, McGraw-Hill, pp. 101-230.
- Raven, F.H (2003) Automatic Control Engineering, 4th edition, McGraw-Hill, New York, pp.170-213.
- Rose, R.H (1963). Encyclopedia of Chemical(Universal Oil Product) Technology, Vol. 1, p. 882.
- Smith, J.M and Ness, H. C. (1999). Introduction to Chemical Engineering, 3rd edition, McGraw Hill, pp. 20-393.
- Strout, K. A. (1995). Engineering Mathematics, 4th edition, 1995, Macmillian Publisher, pp.50-72.
- Wayne, B. B. (2006). Process Control, Modeling Design and Simulation, 8th edition, Prentice Hall of India Private Limited, pp. 197-200.
- Zhang, J and Li, A. (2004). A Correlation of Steel Corrosion in Non-Isothermal LBE Loop Systems, *Journal of Nuclear Science and Technology*, VOL.41 No. 3, pp 260-264
- Zhang, J; Li, N and Cheng, Y. (2005). Dynamics of High Temperature Oxidation Accompanied by Scale Removal and Implication for Technological Application, *Journal of Nuclear Materials*, Vol. 40, No.3, pp. 220-231.
